Optimal random deposition of interacting particles

Adrian Baule[1]
[1] *School of Mathematical Sciences, Queen Mary University of London, London E1 4NS, UK* *

Irreversible random sequential deposition of interacting particles is widely used to model aggregation phenomena in physical, chemical, and biophysical systems. We show that in one dimension the exact time dependent solution of such processes can be found for arbitrary interaction potentials with finite range. The exact solution allows to rigorously prove characteristic features of the deposition kinetics, which have previously only been accessible by simulations. We show in particular that a unique interaction potential exists that leads to a maximally dense line coverage for a given interaction range. Remarkably, this distribution is singular and can only be expressed as a mathematical limit. The relevance of these results for models of nucleosome packing on DNA is discussed. The results highlight how the generation of an optimally dense packing requires a highly coordinated packing dynamics, which can be effectively tuned by the interaction potential even in the presence of intrinsic randomness.

The deposition of particles on a substrate is a ubiquitous phenomenon in science and engineering [1]. From a theoretical perspective, the deposition dynamics is widely modelled in terms of a random sequential adsorption (RSA) process, which represents a paradigmatic adsorption mechanism [2]. Since Renyi's seminal work on the "car parking problem" (the RSA of equal line segments in $1d$) [3, 4], RSA models and their variants have been successfully used to model polymer and colloid adsorption on surfaces [5–7] and are also relevant in other contexts such as the compactification of granular matter [8, 9], genome sequencing [10], and nucleosome packing on DNA [11–15]. However, in almost all studies, particles have been assumed to interact solely through hard-core steric exclusion, despite the fact that realistic particles typically interact with a soft-core potential due to their internal structure [16]. In fact, including soft particle interactions significantly alters the filling behaviour and can account, e.g., for the observed rapid filling of nucleosomes on DNA [14, 15, 17]. In this work, we derive the exact time dependent solution of $1d$ continuum RSA processes with arbitrary finite-range particle interactions using an iterative approach. This method also provides the exact general solution of the related RSA of polydisperse particles, which has been an open problem since the 1960s for the continuum $1d$ case [18–23], notwithstanding specific scaling solutions that have been found [20–22, 24]. The exact solution allows in particular to address the fundamental question how the packing density of the deposition process can be optimized by tuning the particle interactions or size distribution. Remarkably, the solution reveals that a unique interaction potential/size distribution exists that leads to a maximally dense coverage of the line, which is approached as $\sim t^{-\nu}$, where $\nu \to 0^+$ is infinitesimally small.

In RSA, a particle's position is selected with uniform probability over the domain and it is then placed sequentially if there is no overlap with any previously placed particles. Particles are not able to move or reorient once being placed. In order to parametrize the RSA dynamics of equal particles by a rate equation in $1d$, we define an interval x as the distance between the centers of two nearest-neighbor particles on the line of length L and introduce $N(x,t)\mathrm{d}x$ as the number of intervals with size $\in [x, x+\mathrm{d}x]$ at time t. The definition of x implies that $\int_0^L \mathrm{d}x\, x\, N(x,t) = L$ is a conserved quantity of the dynamics for all t. The interval distribution $p(x,t)$ is defined as $p(x,t) = \frac{\lambda}{L} N(x,t)$, where λ is a characteristic length scale associated with the particles [44]. Scaling length as $x \to x/\lambda$ and considering the limit $L \to \infty$, the time evolution of $p(x,t)$ is exactly described by the master equation

$$\frac{\partial}{\partial t} p(x,t) \;=\; -\psi(x)p(x,t) + 2\int_x^\infty \mathrm{d}y\, \Omega(x,y)p(y,t), \quad (1)$$

where the first term on the rhs describes the destruction of intervals of length x and the second term the creation. $\Omega(x,y)$ is the probability per unit time that a particle is placed inside an interval of length y, thus creating an interval of length x. The factor 2 stems from the fact that in $1d$ there are always two ways of doing this for a given y (x is either the distance of the newly inserted particle with the existing left or right particle). The destruction term is accordingly governed by the function $\psi(x) = \int_0^x \mathrm{d}u\, \Omega(u,x)$. The interval distribution satisfies $\int_0^\infty \mathrm{d}x\, x\, p(x,t) = 1$ for all t. Moreover, since one particle is associated with every interval x, the integral $\int_0^\infty \mathrm{d}x\, p(x,t) = n(t)$ equals the number density of particles. The requirement of an initially empty line thus leads to the initial condition $n(0) = 0$ or $p(x,0) = 0$. From Eq. (1) this implies that $\lim_{t\to 0} \frac{\partial}{\partial t} p(x,t) = 0$, but one can show that $\lim_{t\to 0} \frac{\partial^2}{\partial t^2} p(x,t) > 0$ such that $n(t)$ monotonically increases with time. The key quantity of interest is the line coverage (packing density)

$$\phi(t) = 1 - \int_\sigma^\infty \mathrm{d}x\, (x-\sigma)\, p(x,t), \quad (2)$$

where σ denotes the effective size (diameter) of a particle (see below). Note that for soft particles $n(t)$ and

*Electronic address: a.baule@qmul.ac.uk

$\phi(t)$ have very different long-time behaviours: while the jamming density $\phi_J = \lim_{t\to\infty}\phi(t) \le 1$, $n(t)$ can diverge as $t \to \infty$, since particles can be absorbed inside existing particles. By contrast, for hard particles they are directly related as $\phi(t) = \sigma n(t)$ [6].

The simplest example of a deposition process governed by Eq. (1) is Renyi's seminal car parking problem, where particles only interact by steric repulsion [3, 4, 25, 26]. In this case, an exact solution for $p(x,t)$ is known and yields as hallmark features $\phi_J = 0.7475... \equiv \phi_R$ with the algebraic asymptotic approach $\phi_J - \phi(t) \sim t^{-1}$. Other models of the form Eq. (1) have been solved for specific Ω that lead to scale invariant solutions p, e.g, RSA [20–22] and fragmentation processes [27–30]. In the following, an exact analytical solution is derived much more generally without the requirement of scale invariance.

For interacting particles we assume the form

$$\Omega(x,y) = k_+\,\omega(x)\omega(x-y), \tag{3}$$

where the adsorption rate k_+ sets the time scale (set to unity) and $\omega(x)$ describes the modification in the rate due to particle overlap. The particle interactions are constrained as follows: (i) $\omega(x) = 1$ for $x \ge a$, i.e., a is the finite range of the interaction; and (ii) $\omega(x) = 0$ for $x \le \Delta$, i.e., Δ is the hard-core exclusion volume of a particle. Clearly, (i,ii) are satisfied for almost all realistic particle models at least to a good approximation. The hard particle case of Renyi is obtained as $\omega(x) = \Theta(x-a)$ with $\Delta = a$, where $\Theta(x)$ denotes the Heaviside step function. For soft particles $\omega(x)$ interpolates between 0 and 1 (see Fig. 2a).

The properties (i,ii) of $\omega(x)$ constrain the form of ψ and $\Omega(x,y)$ as follows (Supplement Sec. I):

$$\Omega(x,y) = \omega(y-x), \qquad x > a \tag{4}$$
$$\psi(x) = 0, \qquad x \le 2\Delta \tag{5}$$
$$\psi(x) = x - 2\sigma, \qquad x \ge 2a \tag{6}$$

where $\sigma = a - \int_\Delta^a \mathrm{d}u\,\omega(u)$ can be interpreted as the effective size of a particle.

With Eqs. (4–6) the solution of Eq. (1) can be found as follows. For $x \ge 2a$, Eq. (1) simplifies to

$$\frac{\partial}{\partial t}p = -(x-2\sigma)p + 2\int_{x+\Delta}^{\infty}\mathrm{d}y\,\omega(y-x)p(y,t). \tag{7}$$

Crucially, Eq. (7) admits an exact solution of the form

$$p_0(x,t) = t^2F(t)e^{-(x-2\sigma)t}. \tag{8}$$

Substituting this ansatz in Eq. (7) and solving the resulting ODE for $F(t)$ with the initial condition $F(0) = 1$ yields

$$F(t) = \exp\left[-2\int_0^t \mathrm{d}s\frac{1-\int_\Delta^a \mathrm{d}u\,\rho(u)e^{-us}}{s}\right], \tag{9}$$

where we introduce $\rho(x) = \omega'(x)$. We now distinguish the two cases $\Delta > 0$ and $\Delta = 0$.

The key observation is that for a finite excluded volume $\Delta > 0$, we directly obtain a solution in the regime $2a - \Delta \le x \le 2a$ (denoted by p_1) even though ψ is non-linear: property (ii) of $\omega(x)$ enforces the constraint $\Theta(y-x-\Delta)$ in the integral in Eq. (1), which thus only integrates over p_0, i.e., the master equation for $2a - \Delta \le x \le 2a$ is

$$\frac{\partial}{\partial t}p_1(x,t) = -\psi(x)p_1(x,t) + 2\int_{x+\Delta}^{\infty}\mathrm{d}y\,\Omega(x,y)p_0(y,t). \tag{10}$$

This simple first-order ODE with inhomogeneity can be directly integrated:

$$p_1(x,t) = 2\int_0^t \mathrm{d}s\,e^{-\psi(x)(t-s)}\int_{x+\Delta}^{\infty}\mathrm{d}y\,\Omega(x,y)p_0(y,t). \tag{11}$$

Likewise, the solution in the range $2a-2\Delta \le x \le 2a-\Delta$ can be obtained by integration over p_0 and p_1, and so on. Overall, we thus decompose the interval distribution as

$$p(x,t) = \begin{cases} p_0(x,t), & x \ge 2a \\ p_1(x,t), & 2a-\Delta \le x < 2a \\ \vdots & \\ p_j(x,t) & 2a-j\Delta \le x < 2a-(j-1)\Delta \\ \vdots & \\ p_n(x,t) & 2\Delta \le x < 2a-(n-1)\Delta \\ p_{n+1}(x,t) & \Delta < x < 2\Delta \end{cases} \tag{12}$$

Due to the excluded volume, $p(x,t) = 0$ for $x \le \Delta$. We introduce the shorthand notation $\Theta_j(x)$ to separate the different x ranges in Eq. (12) and write $p(x,t) = \sum_{j=0}^{n+1}\Theta_j(x)p_j(x,t)$. The solutions $p_1, ..., p_{n+1}$ are thus obtained by solving the ODE Eq. (1) for each range leading to

$$p_j(x,t) = 2\int_0^t \mathrm{d}s\,e^{-\psi(x)(t-s)}\int_{x+\Delta}^{\infty}\mathrm{d}y\,\Omega(x,y)\times \times\sum_{i=0}^{j-1}\Theta_i(y)p_i(y,s), \qquad j = 1,...,n \tag{13}$$

and

$$p_{n+1}(x,t) = 2\int_0^t \mathrm{d}s\int_{x+\Delta}^{\infty}\mathrm{d}y\,\Omega(x,y)\sum_{i=0}^{n}\Theta_i(y)p_i(y,s), \tag{14}$$

since $\psi(x) = 0$ for $x \le 2\Delta$. Eqs. (8–14) represent the exact analytical solution of Eq. (1) for finite range interactions and $\Delta > 0$.

When $\Delta \to 0$, we can use a limiting procedure in Eqs. (13,14) or use Eq. (8) in Eq. (1) and separate the

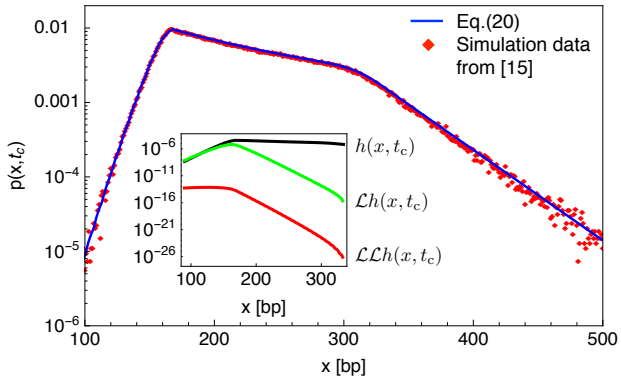

FIG. 1: (Colors online) Comparison of the analytical result Eq. (20) and the numerically obtained interval distribution at cramming onset t_c from simulations of the equilibrium dynamics for the nonlinear potential Eq. (18) [15]. Since the condition $\phi(t_c) = \phi_R$ fixes the time scale k_+, there is no free parameter in the theory. Inset: The first three terms in the series solution Eq. (16), indicating convergence after the first two terms.

integration region. In both cases, the result is

$$\frac{\partial}{\partial t}p_<(x,t) = -\psi(x)p_<(x,t) + 2\int_x^{2a} dy\,\Omega(x,y)p_<(y,t) + 2\int_{2a}^{\infty} dy\,\Omega(x,y)p_0(y,t), \quad (15)$$

where $p_<$ is the interval distribution for the whole range $0 \le x \le 2a$. Using the Duhamel principle, Eq. (15) can be solved by iteration leading to a series solution. We define the compact linear operator $\mathcal{L}f(x,t) = 2\int_0^t ds\, e^{-\psi(x)(t-s)} \int_x^{2a} dy\,\Omega(x,y)f(y,t)$ and obtain the formal solution

$$p_<(x,t) = \frac{1}{1-\mathcal{L}}h(x,t) = h(x,t) + \mathcal{L}h(x,t) + \mathcal{L}\mathcal{L}h(x,t) + ... \quad (16)$$

$$h(x,t) = 2\int_0^t ds\, e^{-\psi(x)(t-s)} \int_{2a}^{\infty} dy\,\Omega(x,y)p_0(y,s) \quad (17)$$

Convergence of this series needs to be established for a given x, t range and Ω.

As an example, where these results can provide novel analytical insight, we consider a model of nucleosome packing on DNA. In [14, 15] genome packaging in eukaryotic cells has been modelled assuming an effective 'softness' of the nucleosomes due to a multitude of internal states with different footprints on DNA [14, 15]. The effective interaction potential has been approximated from in vivo data as [14]

$$V(x) \approx (a-x)\kappa - \log\left[1 + (a-x)\left(1-e^{-\kappa}\right)\right], \quad (18)$$

where $a = 167$ base pairs (bp) is the maximal footprint size and $\kappa = 0.15$ the stiffness per bp. A numerical investigation of the equilibrium kinetics of Eq. (18) exhibits a universal interval distribution independent of the adsorption rate k_+ at a specific time t_c. The time t_c is defined by the condition $\phi(t_c) = \phi_R$ and denotes the onset of 'cramming', where nucleosomes are increasingly squeezed into gaps that are smaller than the maximal footprint size [14, 15]. The dynamics in the cramming regime can be described as follows. In nucleosome packing both adsorption (with rate k_+) and desorption (with rate k_-) occur whereby $k_+ \gg k_-$. Thus in a time regime $\ll 1/k_-$ the equilibrium dynamics is well described by an irreversible RSA process like Eq. (1) [31, 32]. Here, the effect of the interaction potential can be captured by the Boltzmann factor [14, 15]

$$\Omega(x,y) = k_+ \exp\left[-V(x) - V(y-x)\right], \quad (19)$$

setting $k_BT = 1$ and the normalization constant is included in k_+. Since t_c has been observed to be $\ll 1/k_-$, the RSA process applies in the cramming regime and explains immediately the apparent universality of the interval distribution: different k_+ lead to different t_c values, but the resulting $p(x,t_c)$ are all identical, since they are determined at the same ϕ value. In fact, this observation shows that the universality holds not only at cramming onset, but for any fixed ϕ value in the regime $\ll 1/k_-$. It also highlights that the curves $\phi(t)$ for different k_+ are all scaled versions of each other up to times $t \approx 1/k_-$, which is indeed suggested in the numerical results of [15]. Remarkably, with Eqs. (8,16,17) we obtain

$$p(x,t_c) = \begin{cases} p_0(x,t_c), & x \ge 2a \\ (1+\mathcal{L})h(x,t_c), & 0 \le x < 2a \end{cases} \quad (20)$$

which shows perfect agreement with the numerically obtained interval distribution at t_c [15] despite the strong nonlinear character of the interaction potential Eq. (18).

We now want to understand how dense packings on the line can be generated by tuning the interaction potential V assuming $\omega(x) = e^{-V(x)}$ as in Eq. (19). For simplicity, we restrict the discussion to purely repulsive interactions such that $\omega(x)$ is monotonically increasing with $0 \le \omega(x) \le 1$ for $x \in [\Delta, a]$. We then make two key observations: (a) For $\sigma \ge 2\Delta$ the effective size is larger than the minimal separation of two particles, thus the line will eventually be fully covered by particles and $\phi_J = 1$. We thus assume the more interesting case $2\Delta > \sigma$ in the following. (b) For $a > \Delta$ a potential leading to a maximum in ϕ_J must exist. We can conclude this surprising fact from the two limiting forms of ω that satisfy the properties (i,ii) and the repulsive nature (see Fig. 2a). One limit is $\omega(x) = \Theta(x-a)$ (leading to $\sigma = a$) and the other limit is $\omega(x) = \Theta(x-\Delta)$ (leading to $\sigma = \Delta$). However, in both cases we recover $\phi_J = \phi_R$, since ϕ_J is invariant with respect to a single size scale a or Δ on an infinite line. When $a > \Delta$, we have $\phi_J > \phi_R$, so a potential leading to a maximum must exist for a given a. What is the form of this optimal potential?

In order to elucidate this matter, we consider a one-parameter family of potentials that can interpolate be-

tween the two limiting forms of $\omega(x)$ (see Fig. 2a)

$$V(x) = \begin{cases} -\mu \log\left(\frac{x-\Delta}{a-\Delta}\right), & \Delta \le x \le a \\ 0, & x > a \end{cases} \quad (21)$$

where $\mu > 0$. The resulting ϕ_J increases monotonically for larger μ (Fig. 2c). Surprisingly, this suggests that the maximally dense packing is reached when $\omega(x)$ becomes infinitesimally close to the step function limit $\Theta(x-a)$. One can show (Supplement Sec. III) that the interval distribution then converges to the stationary limit $p_s(x) = \Theta(x-a)\Theta(2\Delta - x)\tilde{p}^*(x-a)$, where

$$\tilde{p}^*(z) = 2\int_0^\infty \mathrm{d}t\, t\, \exp\left[-zt - 2\int_0^t \mathrm{d}s \frac{1-e^{-as}}{s}\right], \quad (22)$$

and the corresponding maximal line coverage is

$$\phi_{\mathrm{opt}} = \phi_R + \int_{2\Delta-a}^{a} \mathrm{d}u\, z\, \tilde{p}^*(z). \quad (23)$$

As shown in Fig. 2b, $p_s(x)$ diverges at $x = \sigma = a$ indicating a large number of particle configurations with no empty space between neighbors. The optimal density ϕ^{opt} increases monotonically as a function of a (see inset of Fig. 2c). Note that the limit $\mu \to \infty$ is singular, recovering the Renyi density ϕ_R instead (Supplement Sec. III). Remarkably, Eqs. (22,23) remain valid for any potential for which $\omega(x)$ approaches $\Theta(x-a)$ infinitesimally closely, highlighting that these results are independent of the specific form Eq. (21). This non-trivial property can be understood intuitively. In the $\mu \gg 1$ regime the system behaves initially like the Renyi car parking of hard particles: since $\omega(x)$ is infinitesimally close to $\Theta(x-a)$ all trial configurations with particle overlap are practically rejected until no gaps $x \ge 2a$ remain. Subsequently, the steep decay of $\omega(x)$ prevents that intervals $x < 2a$ are filled with larger than necessary overlaps. The optimal potential thus induces a perfectly hierarchical filling, where all intervals $2\Delta < x < 2a$ are eventually filled, but extremely slowly. In fact, with the previous results and the asymptotic properties of ψ we find that for $\mu \gg 1$ (Supplement Sec. IV)

$$\phi_J - \phi(t) \sim \int_{2\Delta}^{2a-(n-1)\Delta} \mathrm{d}x\, e^{-\psi(x)t} \sim t^{-\nu}, \quad (24)$$

where $\nu = \frac{1}{2\mu+1}$. Nevertheless, Eq. (23) can be verified in a simulation by running the Renyi car parking RSA with length scale a and then considering all intervals $x > 2\Delta$ as filled when evaluating ϕ_J. This indeed yields perfect agreement with the theory (see inset of Fig. 2c).

The iterative solution method can be applied to related interacting particle models such as the continuum RSA of polydisperse particles in $1d$, whose general time-dependent solution has been a long-standing open problem [18–23]. Crucially, this problem can be solved in full generality akin to the interacting particle case for an arbitrary size distribution $\rho(\sigma)$ with support $\sigma \in [\sigma_1, \sigma_2]$

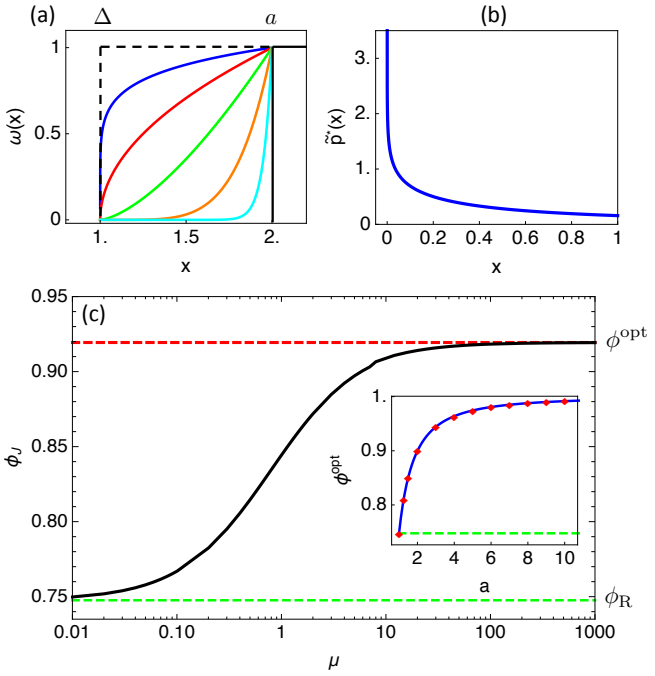

FIG. 2: (Colors online) (a) The two limiting forms of $\omega(x)$: $\Theta(x-\Delta)$ and $\Theta(x-a)$ together with interpolations from the potential Eq. (21). (b) Plot of $\tilde{p}^*(z)$, Eq. (22), the distribution of empty gaps ($z = x - a$) for $t \to \infty$ and $\mu \gg 1$ (here $a = 1$). (c) Plot of ϕ_J resulting from the potential Eq. (21) calculated from the analytical solution Eqs. (8–14) (here $a = 1.4$, $\Delta = 1$). Inset: Plot of ϕ^{opt}, Eq. (23), together with simulation results (here $2\Delta - a = 1$).

(Supplement Sec. V). The solution shows in particular that the exponent of the asymptotic approach is determined by the leading term in the asymptotic expansion of $\rho(\sigma)$ as $\sigma \to \sigma_1$. The widely used assumption that polydispersity generally reduces the exponent by an additional degree of freedom from $\nu = 1/d$ to $\nu = 1/(d+1)$ [2, 6, 33, 34], where d is the spatial dimension, is thus not correct for $d = 1$. A similar result should hold for the RSA of polydisperse spheres in higher dimensions, where the quantitative dependence on ρ has first been observed empirically [35]. Remarkably, the size distribution $\rho(x)$ that leads to a maximal line coverage yields the same interval distribution and optimal density as in the interacting particle case, given by Eqs. (22,23), where now $\sigma_1 = 2\Delta - a$ and $\sigma_2 = a$ (Supplement Sec. V).

The RSA of interacting particles coresponds to a cooperative RSA problem, where adsorption rates depend on the local environment of the particle with a given range [2]. Cooperative RSA problems have long been studied on discrete lattices, for which exact results are available for M-mers (particles occupying M sites) with cooperativity of range-1 [31, 36, 37], range-M [38, 39], and arbitrary finite range-R [40]. From such discrete models, the continuum equivalent is obtained in the limit of $M \to \infty$. However, performing such a limit in the gen-

eral case of M-mers with general range-R cooperativity, which could be mapped onto the continuum RSA of interacting particles, is non-trivial and left for future work. Further applications of the exact results in the context of nucleosome packing models would be highly interesting. The empirically obtained potential Eq. (18), e.g., might represent an optimal trade-off between achieving a high coverage and a fast filling dynamics on time scales relevant for biological function. To this end not only ϕ_J but the dynamics of $\phi(t)$ needs to be explored in the space of possible potentials. In [41], cold atoms that are excited to high-lying Rydberg states are shown to fill up excitation levels akin to a classical deposition process, where atoms interact through a highly nonlinear potential with excluded volume [42]. The analytical solution obtained here could provide important deeper insight into such cold atom excitations, which would be readily realizable in experiments.

Acknowledgments

AB gratefully acknowledges funding under EPSRC grant EP/L020955/1 and helpful discussions with R. Gutiérrez, J. P. Garrahan, and I. Lesanovsky. AB thanks B. Osberg, J. Nübler, and U. Gerland for sharing the simulation data of Fig. 4A in [15].

[1] M. Elimelech, *Particle deposition and aggregation: measurement, modelling, and simulation* (Butterworth-Heinemann, 1995).
[2] J. W. Evans, Rev. Mod. Phys. **65**, 1281 (1993).
[3] A. Rényi, Publ. Math. Inst. Hung. Acad. Sci. **3**, 109 (1958).
[4] A. Renyi, Sel. Trans. Math. Stat. Prob. **4**, 205 (1963).
[5] J. Feder and I. Giaever, J. Colloid Interface Sci. **78**, 144 (1980).
[6] J. Talbot, G. Tarjus, P. V. Tassel, and P. Viot, Colloids Surf. A **165**, 287 (2000).
[7] A. Cadilhe, N. A. M. Araújo, and V. Privman, J. Phys. Condens. Matter **19**, 065124 (2007).
[8] E. R. Nowak, J. B. Knight, E. Ben-Naim, H. M. Jaeger, and S. R. Nagel, Phys. Rev. E **57**, 1971 (1998).
[9] G. Tarjus and P. Viot, Phys. Rev. E **69**, 011307 (2004).
[10] J. C. Roach, V. Thorsson, and A. F. Siegel, Genome Research **10**, 1020 (2000).
[11] R. D. Kornberg and L. Stryer, Nucleic Acids Research **16**, 6677 (1988).
[12] P. Ranjith, J. Yan, and J. F. Marko, Proc. Natl. Acad. Sci. U.S.A. **104**, 13649 (2007).
[13] R. Padinhateeri and J. F. Marko, Proc. Natl. Acad. Sci. U.S.A. **108**, 7799 (2011).
[14] W. Möbius, B. Osberg, A. M. Tsankov, O. J. Rando, and U. Gerland, Proc. Natl. Acad. Sci. U.S.A. **110**, 5719 (2013).
[15] B. Osberg, J. Nuebler, P. Korber, and U. Gerland, Nucleic Acids Research **42**, 13633 (2014).
[16] A. Baule, F. Morone, H. J. Herrmann, and H. A. Makse, Rev. Mod. Phys. **90**, 015006 (2018).
[17] B. Osberg, J. Nuebler, and U. Gerland, Phys. Rev. Lett. **115**, 088301 (2015).
[18] P. E. Ney, Ann. Math. Stat. **33**, 702 (1962).
[19] J. P. Mullooly, J. Appl. Probab. **5**, 427 (1968).
[20] P. L. Krapivsky, J. Stat. Phys. **69**, 135 (1992).
[21] N. V. Brilliantov, Y. A. Andrienko, P. L. Krapivsky, and J. Kurths, Phys. Rev. Lett. **76**, 4058 (1996).
[22] N. Brilliantov, Y. Andrienko, and P. Krapivsky, Physica A **239**, 267 (1997).
[23] D. J. Burridge and Y. Mao, Phys. Rev. E **69**, 037102 (2004).
[24] M. K. Hassan, Phys. Rev. E **55**, 5302 (1997).
[25] J. K. Mackenzie, J. Chem. Phys. **37**, 723 (1962).
[26] B. Widom, J. Chem. Phys. **44**, 3888 (1966).
[27] R. M. Ziff and E. D. McGrady, J. Phys. A **18**, 3027 (1985).
[28] Z. Cheng and S. Redner, Phys. Rev. Lett. **60**, 2450 (1988).
[29] Z. Cheng and S. Redner, J. Phys. A **23**, 1233 (1990).
[30] M. M. R. Williams, Aerosol Sci. Technol. **12**, 538 (1990).
[31] I. R. Epstein, Biopolymers **18**, 765 (1979.
[32] I. R. Epstein, Biopolymers **18**, 2037 (1979.
[33] G. Tarjus and J. Talbot, J. Phys. A **24**, L913 (1991).
[34] Z. Adamczyk, B. Siwek, M. Zembala, and P. Weroński, J. Colloid Interface Sci. **185**, 236 (1997).
[35] P. Meakin and R. Jullien, Phys. Rev. A **46**, 2029 (1992).
[36] J. González, P. Hemmer, and J. Høye, Chem. Phys. **3**, 228 (1974).
[37] E. A. Boucher, Faraday Trans. **69**, 1839 (1973).
[38] N. O. Wolf, J. W. Evans, and D. K. Hoffman, J. Math. Phys. **25**, 2519 (1984).
[39] B. Mellein, J. Math. Phys. **27**, 1839 (1986).
[40] J. W. Evans, J. Phys. A **23**, 2227 (1990).
[41] R. Gutiérrez, J. P. Garrahan, and I. Lesanovsky, Phys. Rev. E **92**, 062144 (2015).
[42] I. Lesanovsky and J. P. Garrahan, Phys. Rev. Lett. **111**, 215305 (2013).
[43] A. Baule, Phys. Rev. Lett. **119**, 028003 (2017).
[44] For hard particles λ would be identified as the size of the particles. For interacting (soft) particles, λ could be identified as the interaction range, effective size, or hard core of the particles.